All-optical switch based on beam cross-cleaning effect in graded-index multimode fiber

Fabio Mangini, Mario Ferraro, Mario Zitelli, Yifan Sun, Katarzyna Krupa, Yann Leventoux, Sebastien Fevrier, Alessandro Tonello, Vincent Couderc, Stefan Wabnitz

All-optical switch based on beam cross-cleaning effect in graded-index multimode fiber

Fabio Mangini
Department of Information Engineering, Electronics and Telecommunications
Sapienza University of Rome
Via Eudossiana 18, Rome, Italy
fabio.mangini@uniroma1.it

Mario Ferraro
Department of Information Engineering, Electronics and Telecommunications
Sapienza University of Rome
Via Eudossiana 18, Rome, Italy
mario.ferraro@uniroma1.it

Mario Zitelli
Department of Information Engineering, Electronics and Telecommunications
Sapienza University of Rome
Via Eudossiana 18, Rome, Italy
mario.zitelli@uniroma1.it

Yifan Sun
Department of Information Engineering, Electronics and Telecommunications
Sapienza University of Rome
Via Eudossiana 18, Rome, Italy
yifan.sun@uniroma1.it

Katarzyna Krupa
Institute of Physical Chemistry Polish Academy of Sciences
Marcina Kasprzaka 44/52, 01-224
Warsaw, Poland
kkrupa@ichf.edu.pl

Yann Leventoux
XLIM Research Institute
University of Limoges, UMR CNRS
123 Avenue Albert Thomas,
87000 Limoges, France
yann.leventoux@unilim.fr

Sebastien Fevrier
XLIM Research Institute
University of Limoges, UMR CNRS
123 Avenue Albert Thomas,
87000 Limoges, France
sebastien.fevrier@unilim.fr

Alessandro Tonello
XLIM Research Institute
University of Limoges, UMR CNRS
123 Avenue Albert Thomas,
87000 Limoges, France
alessandro.tonello@unilim.fr

Vincent Couderc
XLIM Research Institute
University of Limoges, UMR CNRS
123 Avenue Albert Thomas,
87000 Limoges, France
vincent.couderc@xlim.fr

Stefan Wabnitz
Department of Information Engineering, Electronics and Telecommunications
Sapienza University of Rome
Via Eudossiana 18, Rome, Italy
stefan.wabnitz@uniroma1.it

***Abstract*—We introduce the concept of beam all-optical spatial beam switching in graded-index multimode fibers. This consists of seeding a bell-shaped spatial profile to a laser beam at the output of the fiber by exploiting the nonlinear coupling between the modes of the two input beams. Remarkably, we demonstrate that even a weak-control signal allows for improving the spatial profile of a highly multimode intense signal. The device proposed herein will be easily integrated in state-of-the-art optical networks, and will find application in the fields of space-division-multiplexed telecommunication and of multimode fiber lasers.**

***Index Terms*—Spatial beam self-cleaning, nonlinear optics, thermodynamic model, optical switch**

We acknowledge the support of the European Research Council (ERC) under the EU HORIZON2020 Research and Innovation Program (740355), the Italian Ministry of University and Research (R18SPB8227), by Sapienza University of Rome (RG12117A84DA7437), the EU HORIZON2020 Marie Skłodowska-Curie program (713694), and the French research national agency (ANR-18-CE080016-01, ANR-10-LABX-0074-01).

I. Introduction

Optical communications based on multimode fiber (MMFs) started only a decade after the invention of the laser in 1965. In particular, the introduction of MMFs was designed to overcome all of the intrinsic limitations of singlemode fibers (SMFs), e.g., their small mode area and low damage threshold. Indeed, the possibility of exciting and propagating a multitude of modes unlocks a new degree of freedom (i.e., that given by the spatial overlap among the modes), which was inaccessible for SMFs [1]. This makes MMFs the most suitable candidates for applications in space-division-multiplexed telecommunications. Whereas, from a fundamental point of view, MMFs permit to investigate the fascinating behavior of complex systems, whose evolution is governed by the nonlinear interactions among multiple modes [2]. Moreover, the high damage threshold of MMFs allows for up-scaling both the pulse energy and the average power from fiber lasers.

Nevertheless, since the beginning of the 80s, SMFs have been largely preferred for building up optical fiber networks, owing to their much larger bandwidth (due to the absence of modal dispersion) and high-quality output beams. As a matter of fact, the low spatial beam quality resulting from multimode interference makes it challenging to use MMFs for building up fiber lasers. As a consequence, to date, SMFs are largely dominant in nearly all fields of application of optical fibers.

Only in recent years, also thanks to the introduction of laser sources emitting ultra-short and high-power pulses, research interest in MMFs has experienced a revival. Indeed, such lasers allow for discovering novel nonlinear phenomena, such as supercontinuum generation [2], [3] and multiphoton effects [4], [5], which are particularly effective when combined with complex beam propagation in MMFs.

Among these new phenomena, the most relevant for applications is probably the so-called spatial beam self-cleaning (BSC) effect. This consists of the transformation of the beam profile at the output of a graded-index (GRIN) MMF from spatially disordered pattern to a bell-shaped beam [6]. Being driven by the Kerr effect, BSC is obtained whenever the peak power of a laser beam at the fiber input overcomes a certain threshold value, say, P_{thr}. In Fig. 1a, the occurrence of BSC is shown when the laser beam is injected parallel to the fiber axis into the fiber center, i.e., as it is conventionally obtained [7]. However, BSC has been achieved even with tilted geometries [8].

Moreover, it has been demonstrated that the bell-shape of the beam corresponds to a spontaneous rearrangement of the mode occupancy during the propagation, according to the Rayleigh-Jeans (RJ) law [9]. Indeed, BSC can be described as a phenomenon of classical wave thermalization [9], [10]. This is depicted in Fig. 1b, where the white histogram that overlaps with the beam image represents the mode energy distribution. As it can be seen, at the occurrence of BSC, the fundamental mode is the most populated one (in agreement with the RJ distribution). Whereas higher-order modes (HOMs) have a smaller, albeit nonnegligible, population occupancy. Within the thermodynamics framework, it is easy to comprehend several features of BSC that were not fully understood before. For example, it is possible to explain why the values of P_{thr} are higher when the laser beam is injected with a tilt angle ϑ, when compared with threshold power that is needed for an aligned laser-fiber coupling geometry [8]. This is because the mode distribution at the fiber input is already rather similar to the RJ law when injecting a Gaussian beam straight on-axis (roughly one may notice that a BSC beam is quite similar to a Gaussian beam). Thus, beam propagation commences from a configuration which is already similar to that corresponding to the equilibrium state. To the contrary, in the presence of a tilt angle ϑ, the input mode distribution is not so similar to the RJ law, as it occurs in the previous case. As a consequence, either a longer propagation distance (that plays the role of the "time" that the system needs to thermalize) or a higher power (that rules the exchange of energy among the modes) is needed in order to reach thermodynamic equilibrium, i.e. to achieve BSC.

Therefore, with a slightly tilted geometry, it is possible to obtain a speckled output beam with the same (or even higher) power that the value which is needed for triggering BSC in a straight configuration (see Fig. 1c). To such an output beam, corresponds a mode distribution that remains far from the RJ law, since the fundamental mode is not the most populated one (see Fig. 1d).

Starting from this observation, we propose and experimentally demonstrate that a beam with a bell-shaped spatial profile at the fiber output may result from the co-propagation of two beams, only one of which experiences BSC. The latter, which we dub A beam, is injected straight into the fiber center (as in Fig. 1a). Whereas, the beam whose standalone propagation produces speckles is injected within a tilt angle ϑ (as in Fig. 1c). From now on, we will label such a beam with the letter B. Finally, we will talk about $A+B$ beam when simultaneously injecting both A and B beams (cfr. Fig. 1e). At a fixed ratio between the power of the A and B beams, their combination still leads to a speckled output profile, if insufficient total power is provided at the fiber input. Whereas, a cleanup of the output combined beam, i.e., a substantial increase of its brightness and quality, occurs whenever the power of $A+B$ overcomes a certain threshold value (see Fig. 1g). Note that, under this condition, the propagation of the sole B beam still produces a speckled output beam. Therefore, the transformation of the $A+B$ beam output profile from speckles to a bell-shape is, in fact, induced by the coherent interaction between A and B beams. In the following, we will refer to such a transformation as cross-beam-cleaning (CBC).

Remarkably, we found that CBC occurs even when the power of the A beam is tenfold smaller than that of the B beam. Such a result, which is not shown in this abstract, but can be found in Ref. [11], means that CBC can be used to demonstrate an efficient all-optical switching mechanism based on MMFs. Therefore, in the following, we will refer to the occurrence of CBC as switch-on configuration; analogously, a speckled output of the $A+B$ beam will be indicated as switch-off configuration.

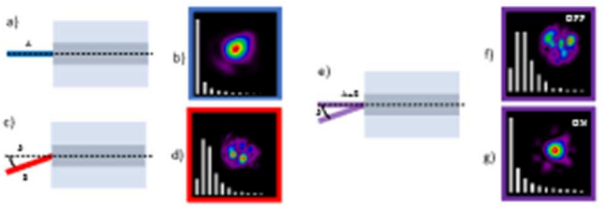

Fig. 1. Sketch of the all-optical spatial beam switching effect in MMF. (a) A beam injected straight into the fiber center. (b) Corresponding output spatial profile at the occurrence of BSC. The white histogram represents the occupancy of the modes, grouped and sorted according to their propagation constants. (c) B beam injected in the fiber center within an angle ϑ with respect to the fiber axis. (d) Corresponding output spatial profile, for an input power lower than P_{thr}. (e) Sketch of the $A+B$ beam injection conditions. (f,g) Corresponding output beam profile and associated mode occupancy histogram at powers below (f) and above (g) the threshold for the occurrence of CBC.

II. Experimental Setup

The experimental setup for the proof-of-principle demonstration of CBC is shown in Fig. 2. In particular, we split the figure into two parts. In Fig. 2a, we show the optical components used for reproducing the injection conditions as in Fig. 1e. Whereas, in Fig. 2b, we show the analysis system for determining the mode distribution at the fiber output.

The simultaneous injection of two beams is obtained by means of an optical system that resembles a Michelson interferometer. However, with respect to the latter, the beam splitter is replaced by a polarizing beam splitter (PBS). This difference means that the two arms are orthogonally polarized, thus allowing to maximize the input power, since no interference between the A and B beams occurs.

We used an Yb-laser source (Light Conversion PHAROS-SP-HP) emitting pulses of 2 ps at 1030 nm, which are linearly polarized. For this reason, both arms of the interferometer-like setup are equipped with a quarter waveplate. The latter is needed, in order to allow the beam to reach the fiber. In fact, in the absence of these waveplates, light would be reflected back to the laser source, due to the polarization-dependent transmission and reflection properties of the PBS. The ratio between the power of the A and the B beams is fixed by the orientation angle of the $\lambda/2$ waveplate, which is placed ahead of the PBS. Whereas the power of the $A+B$ beam is varied by means of a variable attenuator, which is placed in front of the laser source. Finally, the mirrors in both arms can be tilted, in order to vary the coupling conditions between the laser and the MMF. Note that the system must ensure that both A and B beams are injected into the fiber center. The presence of an offset with respect to the fiber axis, in fact, will provide the beam with an orbital angular momentum [10]. The latter is a conserved quantity upon propagation in cylindrical waveguides, such as MMFs. Thus, the equilibrium distribution will no longer be the standard RJ law, since an extra conservation law must be considered when describing the thermodynamic equilibrium condition [10].

At the fiber output, the beam is collimated by means of a microlens (L_1). In combination with a second lens (L_2), this forms an afocal system which reproduces the field at the fiber output facet onto the reflecting surface of a spatial light modulator (SLM, Hamamatsu LCOS- X15213), within a magnification given by the ratio between the focal lengths of L_2 and L_1. In between the two lenses, we placed a linear polarizer (LP) and a bandpass filter (BPF at 1030±10 nm), in order to avoid spectral broadening caused by self-phase modulation. As a matter of fact, the SLM requires to operate with monochromatic waves with a linear state of polarization. Finally, we added a half-waveplate ($\lambda/2$, which allows for maximizing the power that reaches the SLM. Thus, during propagation, the beam polarization state has a non-trivial evolution [12]. The SLM is used for encoding a phase mask on the beam, whose Fourier transform (made by the lens L_3) is imaged onto a CCD camera (Gentec Beamage-4M-IR). Such a holographic system permits to determine the mode composition of the beam at the fiber output, following the procedure described in Ref. [13]. Roughly, our mode decomposition method can be described as follows. The CCD camera acquires the pattern emerging from the interference of the beam at the fiber output with the phase mask introduced by the SLM. These phase masks are made in order to encode information about both the intensity and phase associated with each mode that composes the beam at the fiber output. In this way, by collecting a set of images captured by the camera, we are able to fully determine the mode composition of a given output beam.

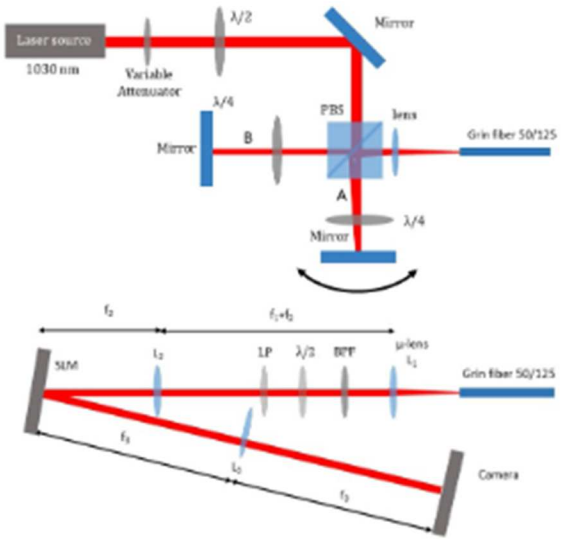

Fig. 2. Sketch of the experimental setup at the input (top) and output (bottom) of the MMF.

III. Results

The demonstration of the all-optical switching effect in the MMF is illustrated in Fig. 3. In particular, in Fig. 3a and b, we report the results relative to the switch-off and the switch-on configurations, respectively, when the power ratio between the A and the B beam is equal to 2, and $\vartheta \simeq 2°$. Each sub-figure shows a comparison between the measured beam intensity profile at the fiber output (left panel), and its reconstruction (right panel), which is calculated by starting from the measurement of the amplitude and phase of the fiber modes, when injecting the sole A beam (top row), the sole B beam (mid row), and the combined $A+B$ beam (bottom row), respectively. As it can be seen, in all cases the reconstructed beam intensity profiles are remarkably similar to what is measured by the camera. This proves the validity of our mode decomposition method.

The measured mode occupancy corresponds to the images in Figs. 3a,b and in Figs. 3c,d. The mode distribution in the switch-on and switch-off configurations is quite different. In particular, in the switch-off configuration, some of the HOMs

are more populated than the fundamental mode, for both the B beam and the $A + B$ beam cases (see cyan and yellow histograms in Fig. 3c, respectively). The other way around, the fundamental mode is the most populated one for the A beam case, while the occupancy of the HOMs quickly drops down (dark blue histogram in Fig. 3c). In particular, the RJ law (solid red line in Fig. 3c) fits well the experimental mode distribution, thus demonstrating the occurrence of beam thermalization.

Note that, as thermal equilibrium is reached, the mode distribution of the A beam barely changes when going to the switch-on configuration, i.e., when increasing the input power (cfr. solid red lines in Figs.3c,d). Besides, in the switch-on configuration, the B beam has not yet thermalized (the mode occupancy in the cyan histogram in Fig. 3d does not decrease monotonically with the increase of the propagation constant). Finally, although it has acquired a bell-shape, we can see that even the $A + B$ beam has not yet reached a thermalized state. As a matter of fact, the third mode group in the yellow histogram in Fig. 3d is more populated than the second mode group. Still, the fundamental mode turns out to be the most populated one.

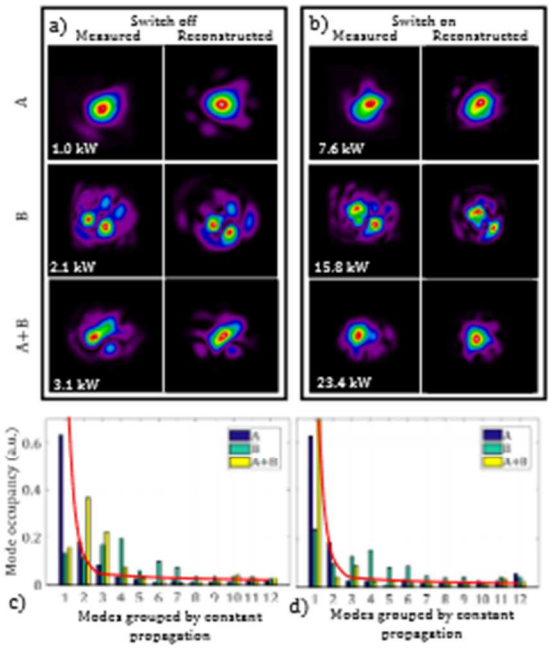

Fig. 3. Experimental results. a,b) Measured output beam profile (left column) and its reconstruction by means of the mode decomposition setup in Fig. 2b (right column). The ratio between the A and the B beam power is equal to 2, whereas the tilt angle is $\vartheta \simeq 2^{\circ}$. d,e) Mode occupancy corresponding to the beam intensity profiles in (a,b).

IV. Conclusions

In conclusion, we introduced and experimentally demonstrated an all-optical switching effect involving multimode beams in optical fibers. The operating mechanism of the switch relies on the nonlinear properties of MMFs, and it is related to Kerr BSC in GRIN fibers. In this contribution we showed that the nonlinear interaction among fiber modes makes it possible to control the spatial profile of a high-power beam by acting only on a low-power beam, which co-propagates in a MMF. Specifically, we observe a CBC effect that consists of providing a bell-shape to the combined beam at the fiber output. The latter was analysed by means of holographic mode decomposition techniques. The experimental results confirm that, similar to the the single-beam self-cleaning effects, bell-shaped beams obtained via CBC also have a dominant fundamental mode contribution.

In perspective, CBC will be particularly useful for designing MMF-based cavities high-power or high-energy fiber laser applications. Finally, in the framework of statistical mechanics of multimode optical systems, our results may pave the way for new developments of the thermodynamics description of beam propagation in MMFs.

References

[1] K. Krupa, A. Tonello, A. Barthélémy, T. Mansuryan, V. Couderc, G. Millot, P. Grelu, D. Modotto, S.A. Babin, and S. Wabnitz, "Multimode nonlinear fiber optics, a spatiotemporal avenue," APL Photonics, vol. 4, no. 11, 110901, 2019.

[2] A. Picozzi, G. Millot, and S. Wabnitz, "Nonlinear virtues of multimode fibre," Nature Photonics, vol. 9, no. 5, pp. 289-291, 2015.

[3] F. Poletti and P. Horak, " Dynamics of femtosecond supercontinuum generation in multimode fibers," Optics Express, vol. 17, no. 8, pp. 6134-6147, 2009.

[4] F. Mangini, M. Ferraro, M. Zitelli, V. Kalashnikov, A. Niang, T. Mansuryan, A. Tonello, V. Couderc, S.A. Babin, F. Frezza, and S. Wabnitz, "Rainbow Archimedean spiral emission from optical fibres," Scientific reports, vol. 11, no. 1, pp. 1-10, 2021.

[5] F. Mangini, M. Ferraro, M. Zitelli, A. Niang, T. Mansuryan, A. Tonello, V. Couderc, A. De Luca, S.A. Babin, F. Frezza, and S. Wabnitz, "Helical plasma filaments from the self-channeling of intense femtosecond laser pulses in optical fibers," Optics Letters, vol. 47, no. 1, pp. 1-4, 2022.

[6] K. Krupa, A. Tonello, B.M. Shalaby, M. Fabert, A. Barthélémy, G. Millot, S. Wabnitz, and V. Couderc, "Spatial beam self-cleaning in multimode fibres," Nature Photonics, vol. 11, no. 4, pp. 237-241, 2017.

[7] Y. Leventoux, G. Granger, K. Krupa, A. Tonello, G. Millot, M. Ferraro, F. Mangini, M. Zitelli, S. Wabnitz, S. Février, and V. Couderc, "3D time-domain beam mapping for studying nonlinear dynamics in multimode optical fibers," Optics Letters, vol. 46 no. 1, pp.66-69, 2021.

[8] E. Deliancourt, M. Fabert, A. Tonello, K. Krupa, A. Desfarges-Berthelemot, V. Kermene, G. Millot, A. Barthélémy, S. Wabnitz, and V. Couderc, "Kerr beam self-cleaning on the LP 11 mode in graded-index multimode fibers," OSA Continuum, vol. 2, pp. 1089-1096, 2019.

[9] F. Mangini, M. Gervaziev, M. Ferraro, D.S. Kharenko, M. Zitelli, Y. Sun, V. Couderc, E.V. Podivilov, S.A. Babin, and S. Wabnitz, "Statistical mechanics of beam self-cleaning in GRIN multimode optical fibers," Optics Express, vol. 30, pp. 10850-10865, 2022.

[10] E.V. Podivilov, F. Mangini, O.S. Sidelnikov, M. Ferraro, M. Gervaziev, D.S. Kharenko, M. Zitelli, M.P. Fedoruk, S.A. Babin, S. Wabnitz, "Thermalization of orbital angular momentum beams in multimode optical fibers," Physical Review Letters, vol 128, 243901, 2022.

[11] M. Ferraro, F. Mangini, Y. Leventoux, A. Tonello, M. Zitelli, Y. Sun, S. Fevrier, K. Krupa, D. Kharenko, S. Wabnitz, and V. Couderc, "Multimode optical fiber beam-by-beam cleanup," arXiv preprint arXiv:2205.13385, 2022.

[12] K. Krupa, G. Garmendia Castañeda, A. Tonello, A. Niang, D.S. Kharenko, M. Fabert, V. Couderc, G. Millot, U. Minoni, D. Modotto, and S. Wabnitz, "Nonlinear polarization dynamics of Kerr beam self-cleaning in a graded-index multimode optical fiber," Optics letters, vol. 44, no. 1, pp. 171-174, 2019.

[13] M.D. Gervaziev, I. Zhdanov, D.S. Kharenko, V.A. Gonta, V.M. Volosi, E.V. Podivilov, S.A. Babin, and S. Wabnitz, "Mode decomposition of multimode optical fiber beams by phase-only spatial light modulator," Laser Physics Letters, vol. 18, no. 1, 015101, 2020.